CLEAN TECHNOLOGY, Vol. 14, No. 4, December 2008, pp. 242~247

청정생산공정기술

초임계 반용매법을 이용한 폴리비닐피롤리돈 미세입자의 제조

신문삼, 김화용*

서울대학교 화학생물공학부
151-744 서울시 관악구 신림동 산56-1

(2008년 8월 25일 접수; 2008년 9월 12일 수정본 접수; 2008년 9월 18일 채택)

Preparation of Poly(*N*-vinyl-2-pyrrolidone) Microparticles Using Supercritical Anti-solvent

Moon Sam Shin and Hwayong Kim*

School of Chemical and Biological Engineering, Seoul National University
San 56-1, Shinlim-dong, Gwanak-gu, Seoul 151-744, Korea

(Received for review August 25, 2008; Revision received September 12, 2008; Revision accepted September 18, 2008)

요 약

화장품, 의약품, 전자소재 분야에서 생체적합, 생분해성 고분자로 널리 사용되는 폴리비닐피롤리돈(PVP)을 에어로젤 용매추출 방법에 의해 미세입자를 제조하였다. 용매로는 이염화메탄을, 반용매로는 초임계 이산화탄소가 사용되었다. 온도, 압력, 이산화탄소 유량, 용액유량의 작업조건에 따라 0.184 - 0.249 μm입자크기를 얻었고, 그 입자크기에 영향을 미치는 초기구형 입자크기와의 상관관계를 규명하였다.

주제어 : 폴리비닐피롤리돈, 반용매, 미세입자, 초임계 유체, 고분자

Abstract : Poly(*N*-vinyl-2-pyrrolidone) (PVP) has been used as biocompatible and biodegradable polymer in cosmetics, pharmaceuticals and electronics. Micro-particles of PVP were produced using an aerosol solvent extraction system (ASES). Dichloromethane (DCM) and supercritical carbon dioxide were used as solvent and antisolvent, respectively. The mean diameter of the obtained polymer particles ranged from 0.184 to 0.249 μm. The relationship between particle size and initial drop size was also considered.

Key words : Poly(*N*-vinyl-2-pyrrolidone), Anti-solvent, Microparticles, Supercritical fluids, Polymer

Introduction

Micro- or nano-sized particles are used in various fields, such as cosmetics, pharmaceuticals, dyes, and electronics. Conventional processes for preparing nano- and micro-particles are crushing, grinding, ball milling, spray drying, and solvent evaporation. These conventional techniques have disadvantages such as thermal and chemical degradation of products, broad particle size distribution[1]. Supercritical fluids are a green solvent for extraction and purification of cosmetics, pharmaceuticals, food supplements and natural products. Using supercritical fluid may overcome the drawbacks of conventional processes. Several processes that use the supercritical fluid for micronization have been studied intensively.

Various processes using supercritical fluids are introduced in review articles[2-5]. Rapid expansion of supercritical solutions

* To whom correspondence should be addressed.
E-mail : hwayongk@snu.ac.kr

(RESS) process consists in dissolving the product in the supercritical fluid and rapidly depressurizing this solution through an adequate nozzle, causing an extremely rapid nucleation of the product into a highly dispersed material. This process is restricted to the products that present a reasonable solubility in supercritical fluid. The concept of the gas anti-solvent (GAS) process consists in decreasing the solvent power of a liquid solvent in which the substrate is dissolved, by saturating it with supercritical fluid, causing the substrate precipitation or recrystallization. The aerosol solvent extraction system (ASES) process consists in atomizing a solution of the substrate in an organic solvent into a precipitator and causing precipitation of product by rapid mass transfer of supercritical fluid and organic solvent.. The ASES process has been applied by various research groups to polymers, pharmaceuticals, and superconductor precursors [6-9]. Most research groups have reported experimental results and the effects of parameters, such as pressure, temperature, and concentration of solution. Mass transfer of supercritical fluids and solvents was also researched[10, 11]. Bristow et al.[12] studied supersaturation in the ASES process. Rantakyla et al. [13] studied the effect of initial droplet size, but they did not consider the effect of other parameters in their analysis. Poly(*N*-vinyl-2-pyrrolidone) (PVP) has been used as biocompatible and biodegradable polymer in cosmetics, pharmaceuticals and electronics.

In this study, micro-particles of PVP were produced using the ASES process to investigate the effect of pressure, temperature and solution flow rate. And the effect of initial droplet sizes on the particle sizes was analyzed.

Mathematical Models

When a liquid jet emerges from a nozzle, it can be broken. Two factors contribute to the jet break up. One is the Reynolds number (*Re*) which is the ratio of inertial force and friction force.

$$\mathrm{Re} = \frac{d_o U_L \rho_L}{\mu_L} \tag{1}$$

where d_o is nozzle diameter (m), U_L is liquid velocity (m/s), ρ_L is liquid density (kg/m^3), and μ_L is liquid viscosity (kg/m s). The other is the Weber number (*We*), which is the ratio of kinetic energy and surface energy.

$$We = \frac{d_0 U_L^2 \rho_L}{\sigma} \tag{2}$$

where σ is interfacial tension (kg/s^2) between gas and liquid.

The Ohnesorge number (*Oh*) is defined by *Re* and *We*:

$$Oh = \frac{\sqrt{We}}{\mathrm{Re}} \tag{3}$$

Larger *Oh* and *Re* indicate the jet stream is better atomized[14].

There are many types of atomizers, and various empirical equations for the initial droplet size are proposed for each type. The most important properties of liquid atomization are surface tension, viscosity and density. For a liquid injected into a gaseous medium, the only thermodynamic property generally considered of importance is the gas density. The significant variables for liquid flow are the velocity of the liquid jet or sheet and the turbulence in the liquid stream. The important gas flow variables are the absolute velocity and the relative gas-to-liquid velocity[14]. In the case of the atomizer used in our experiment (the air-blast type atomizer), the equations that estimate the initial droplet size consist of two terms of relative velocity and surface tension, and have the same form even though parameters of each equation are not same. So the use of these equations is justified for the description of the qualitative relationship between the initial droplet size and the processed particle size. We chose the equation suggested by Lorenzetto and Lefevre[15] to calculate the initial drop size because of the similarity in atomizers.

$$SMD = 0.95\left[\frac{(\sigma m_L)^{0.33}}{\rho_L^{0.37}\rho_G^{0.30}U_{GL}}\right](1+\frac{m_L}{m_G})^{1.70} + 0.13(\frac{\mu_L^2 d_0}{\sigma\rho L})^{0.5}(1+\frac{m_L}{m_G})^{1.70} \tag{4}$$

where the subscript G and L represent air and liquid, and m is flow rate (kg/s). SMD is the acronym of 'Sauter mean diameter' and is defined as follows:

$$SMD = \frac{\sum N_i D_i^3}{\sum N_i D_i^2} \tag{5}$$

where N_i is the number of drops in size range i, and D_i is the middle diameter of size *i*.

According to equilibrium thermodynamics, the interface does not exist above the critical point. Hence, when considering the slow process of carbon dioxide (CO_2) dissolution in a solvent portion above the critical point, the solvent portion might be regarded as an effective droplet without the interface and interfacial tension[10, 11]. However, the interface is often formed very rapidly, and it may be erroneous to analyze this phenomenon with equilibrium thermodynamics[16]. Lengsfeld et al.[17] studied the surface tension of DCM and CO_2 at the critical point of the mixture, and they found that interfacial tension of DCM

Table 1. The mean diameter of PVP particles at various conditions

Experiment number	T (K)	P (MPa)	Solution flow rate (cm^3/min)	CO_2 flow rate (kg/hr)	Conc. (wt %)	Mean particle diameter (μm)
1	313.15	15.0	0.50	2.50	0.50	0.195
2	323.15	15.0	0.50	2.50	0.50	0.233
3	333.15	15.0	0.50	2.50	0.50	0.252
4	343.15	15.0	0.50	2.50	0.50	0.286
5	313.15	13.0	0.50	2.50	0.50	0.216
6	313.15	17.0	0.50	2.50	0.50	0.184
7	313.15	15.0	0.30	2.50	0.50	0.249
8	313.15	15.0	0.40	2.50	0.50	0.230
9	313.15	15.0	0.60	2.50	0.50	0.201
10	313.15	15.0	0.70	2.50	0.50	0.212
11	313.15	15.0	0.50	2.25	0.50	0.203
12	313.15	15.0	0.50	2.75	0.50	0.184

in CO_2 at 8.5 MPa and 308 K approximated to 0.00001 kg/s^2.

Materials and Methods

Materials

PVP (M.W. 55,000) and DCM (min. 99.6%) were supplied from Aldrich. Carbon dioxide (min. 99.5%) was supplied from Korea Industrial Gases.

Apparatus and Methods

A schematic diagram of the semi-continuous ASES apparatus is shown in Figure 1. The volume of the precipitator is about 100 cm^3 and the height is 200 mm. The solution of the copolymer in DCM was pumped with an HPLC pump (Hitachi, L-7110). The liquid CO_2 was pumped with a non-pulsating high-pressure pump (Nihon Seimitsu Kagaku, NP-AX-70). The nozzle was made by Valco Instruments Co. and its inner diameter was 0.127 mm.

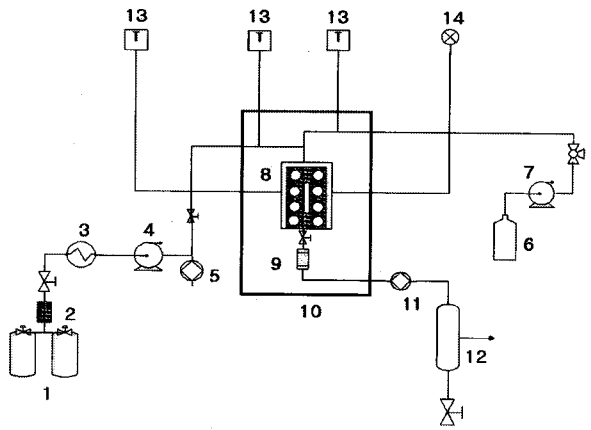

Figure 1. Schematic diagram of the experimental apparatus. (1) carbon dioxide bomb, (2) filter, (3) heat exchanger, (4) high pressure pump, (5) relief valve, (6) solution reservoir, (7) high pressure pump, (8) precipitator, (9) filter, (10) oven, (11) back pressure regulator, (12) separators, (13) thermometer, (14) pressure transducer.

The precipitator was heated in an air convection oven and pressurized with CO_2. The pressure in the precipitator was controlled with a back-pressure regulator (Tescom, 26-1726-24-161). After the temperature and pressure arrived at the set point, the equipment was maintained for about 10 min to achieve a steady-state condition. The solution of copolymer in DCM was pumped through the nozzle. CO_2 was also supplied continuously. CO_2 and the solution were always heated to the precipitator temperature before entering the precipitator. This experiment was conducted for about 60 min, after which the flow of the solution was stopped. The supercritical CO_2 and any residual DCM from the particles were washed out of the precipitator for about 15 min. The copolymer particles were collected in the filter (Swagelok, pore size 0.5 μm). The powder samples were observed with a field emission scanning electron microscope (FE-SEM, JSM-6700F). Feret's diameters of 50 particles[18] per experiment were measured from the FE-SEM images.

Results and Discussion

The experimental conditions and particle size are represented in Table 1. The concentration of PVP solution was 0.5 wt % for all experiments.

Effect of Temperature

The experiments were carried out at temperatures ranging from 313.15 to 343.15 K (experiment runs 1-4 in Table 1). Spherical particles were observed by SEM. As temperature increased, the

mean particle size increased from 0.195 to 0.286 Om and the particles were more agglomerated at higher temperatures.

As temperature was increased, CO_2 density was decreased. As a result, a higher diffusivity and mass transfer are achieved. Consequently, particle size decreases with increasing temperature. On the other hand, particle size was analyzed by dimensionless Weber number[3, 19] defined as the ratio of the deformation and the reformation forces. In general, the higher Weber number it has, the smaller the droplets are as the result of atomization. As the temperature was increased, a lower CO_2 density in the numerator of Weber number caused the lower Weber number. As a result, particle size increases with increasing temperature. Therefore, it can be explained that the effect of atomization dominates that of mass transfer in this experiment.

Effect of Pressure

PVP particles were produced at 13.0, 15.0, and 17.0 MPa (experiment runs 1, 5, 6 in Table 1). As pressure increased, the mean particle size decreased from 0.216 to 0.184 μm. As pressure was increased, CO_2 density and viscosity were increased and diffusivity of CO_2 was decreased. Because, in general, reduced diffusivity and increased viscosity hinder mass transfer between the droplets and the surrounding CO_2, particle size must be increased with increasing pressure. But, increasing pressure led to fine droplets due to increasing aerodynamic force and breakup. Therefore, in this experiment, it can be explained that the effect of atomization on particle sizes is more dominant than that of mass transfer.

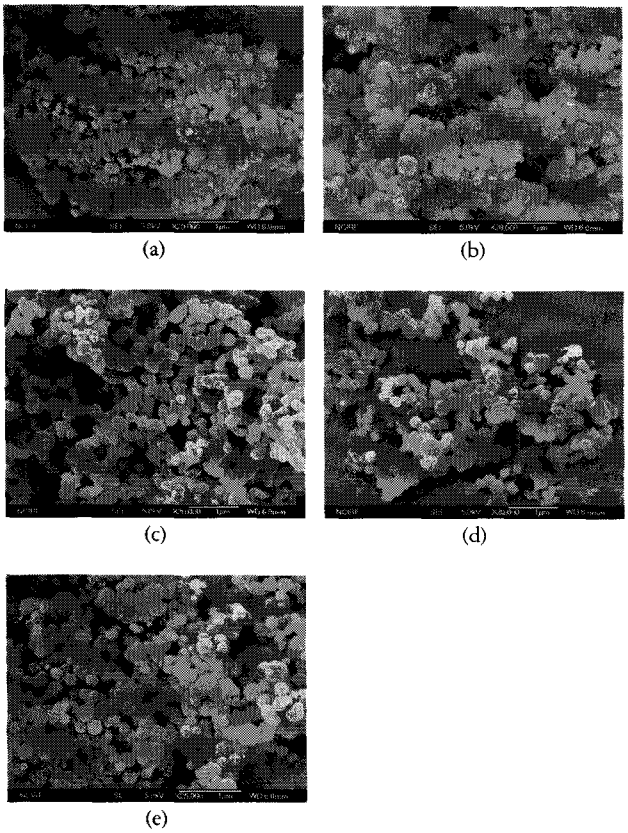

Figure 2. SEM images of PVP particles precipitated with different solution flow rates. (a) 0.3 cm^3/min, (b) 0.4 cm^3/min[15], (c) 0.5 cm^3/min, (d) 0.6 cm^3/min, (e) 0.7 cm^3/min.

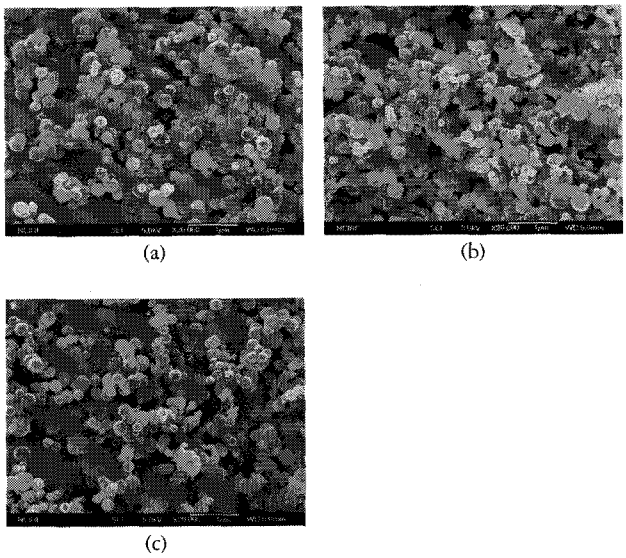

Figure 3. SEM images of PVP particles at various CO_2 flow rates. (a) 2.25 kg/hr, (b) 2.50 kg/hr, (c) 2.75 kg/hr.

Effect of Solution Flow Rate

ASES experiments were performed at liquid solution flow rates ranging from 0.30 to 0.70 cm^3/min (experiment runs 1, 7-10 in Table 1). The SEM images are shown in Figure 2. The mean particle diameter shows V-curve. Eqs. 1-3 shows that low liquid velocity makes Reynolds number and Weber number small and results in non-atomization. If the solution stream is not atomized, the initial drop size would be much bigger than when atomized. It is inferred that the solution flow rates (0.3 and 0.4 cm^3/min) are too low to make the stream fully atomized.

Effect of CO_2 Flow Rate

ASES experiments were performed at CO_2 flow rates raging from 2.25 to 2.75 kg/hr (experiment runs 1, 11, 12 in Table 1). The SEM images are shown in Figure 3. Higher CO_2 flow rates led to smaller mean particle sizes. These results will be analyzed by relation of initial droplet size and mean particle sizes.

Relation of Initial Droplet Size and Particle Size

Thermodynamic equilibrium, mass transfer, and initial droplet size are the main factors affecting the particle sizes produced by ASES. Because thermodynamic equilibrium is affected by

Table 2. Calculated initial droplet size and experimental particle diameter with different solution flow rates and CO_2 flow rates

Experiment run	Solution flow rate (cm^3/min)	CO_2 flow rate (kg/hr)	Calculated initial droplet size (μm)	Experimental particle diameter (μm)
1	0.50	2.50	9.71	0.195
9	0.60	2.50	10.01	0.201
10	0.70	2.50	10.27	0.212
11	0.50	2.25	10.24	0.203
12	0.50	2.75	9.27	0.184

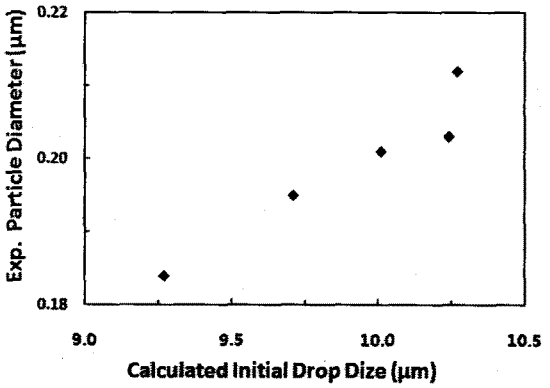

Figure 4. Calculated initial droplet size and experimental particle diameter with different solution flow rates and CO_2 flow rates.

temperature, pressure, and concentration, the calculated initial droplet size was compared to the particle size produced at constant temperature (313.15 K), pressure (15.0 MPa), and concentration (0.5 wt%). The exact mechanisms of mass transfer, nucleation, and particle growth have not yet been reported. However, we expect that there would be no differences in the effects of mass transfer, nucleation, and particle growth on particle formation when the experiments are carried out at the same temperature, pressure, and concentration.

Experiment runs 1 and 7-12 were conducted at the same temperature, pressure, and concentration. The solution flow was not atomized in experiment runs 7 and 8, but experiment runs 1 and 9-12 were atomized. Calculated initial droplet size and experimental particle size, according to the variance of solution flow rate and CO_2 flow rate, are shown in Table 2 and Figure 4. Increase in solution flow rate makes the initial droplet size larger and affects the mean particle size. Decrease in CO_2 flow rate produces the same result. The results show a close linear relationship between the calculated initial drop size and the mean particle size.

Conclusions

Spherical PVP particles were prepared using the ASES process. The mean particle size depended on pressure, temperature, and solution flow rate. As temperature decreased or pressure increased, the mean particle size decreased. If the solution stream was not atomized, then large particle sizes were observed in spite of low solution flow rate. The initial droplet size was calculated and the initial droplet size and particle diameter, at constant temperature and pressure, showed a close linear relationship.

Acknowledgment

This work was supported by the BK21 project of the Ministry of Education of Korea and by the National Laboratory (NRL) Program.

List of symbols

D_i middle diameter of size i
d_0 nozzle diameter
m mass flow rate
N_i number of drops in size range i
U_G gas velocity
U_{GL} velocity difference between gas velocity and liquid velocity
U_L liquid velocity

Greek letters

σ interficial tension
ρ_G gas density
ρ_L liquid density
μ_G viscosity of gas
μ_L viscosity of liquid

Superscript

G gas
L liquid

References

1. Huang, Z., Sun, G.-B., Chiew, Y. C., and Kawi, S., "Formation of Ultrafine Aspirin Particles through Rapid Expansion of Supercritical Solutions (RESS)," *Powder Technol.*, **160**(2), 127-134 (2005).
2. Beckman, E. J., "Supercritical and Near-critical CO2 in Green Chemical Synthesis and Processing," *J. Supercrit. Fluids*, **28**(2-3), 121-191 (2004).
3. Jung, J., and Perrut, M., "Particle Design Using Supercritical Fluids: Literature and Patent Survey," *J. Supercrit. Fluids*, **20**(3), 20, 179-219 (2001).
4. Knez, Z., and Weinder, E., "Particles Formation and Particle Design Using Supercritical Fluids," *Curr. Opin. Solid State Mater. Sci.*, 7(4-5), 353-361 (2003).
5. Yeo, S., and Kiran, E., "Formation of Polymer Particles with Supercritical Fluids: a Review," *J. Supercrit. Fluids*, **34**(3), 287-307 (2005).
6. Reverchon, E., "Supercritical Antisolvent Precipitation of Micro- and Nano-particles," *J. Supercrit. Fluids*, **15**(1), 1-21 (1999).
7. Ghaderi, R., Artursson, P., and Carlfors, J., "A New Method for Preparing Biodegradable Microparticles and Entrapment of Hydrocortisone in DL-PLG Microparticles Using Supercritical Fluids", *Eur. J. Pharm. Sci.* **10**(1), 1-9 (2000).
8. Fusaro, F., Albano, S., and Mazzotti, M., "Enhancement of the Solubilization Behavior of Slightly Soluble Pharmaceuticals by Precipitation of Drug-polymer Co-formulations Using Sc-CO_2 as Antisolvent," Proceedings of the International Symposium on Supercritical Fluids, Orlando (2005).
9. Chattopadhyay, P., and Gupta, R. B., "Supercritical CO_2-based Production of Fullerene Nanoparticles," *Ind. Eng. Chem. Res.*, **39**(7), 2281-2289 (2000).
10. Werling, J. O., and Debenedetti, P. G., "Numerical Modeling of Mass Transfer in the Supercritical Antisolvent Process," *J. Supercrit. Fluids*, **16**(2), 167-181 (1999).
11. Werling, J. O., and Debenedetti, P. G., "Numerical Modeling of Mass Transfer in the Supercritical Antisolvent Process: Miscible Conditions," *J. Supercrit. Fluids*, **18**(1), 11-24 (2000).
12. Bristow, S. T., Shekunov, T., Shekunov, B. Y., and York, P., "Analysis of the Supersaturation and Precipitation Process with Supercritical CO_2," *J. Supercrit. Fluids*, **21**(3), 257-271 (2001).
13. Rantakylä, M., Jäntti, M., Aaltonen, O., and Hurme, M., "The Effect of Initial Drop sSze on Particle Size in the Supercritical Antisolvent Precipitation (SAS) Technique," *J. Supercrit. Fluids*, **24**(3), 251-263 (2002).
14. Lefevre, A. H., Atomization and Sprays, Hemisphere Publishing, New York, 1989.
15. Lorenzetto, G. E., and Lefevre, A. H., "Measurement of Drop Size on a Plane-jet Airblast," *AIAA J.*, **15**(7), 1006-1010 (1977).
16. Dukhin, S. S., Zhu, C., Dave, R., Pfeffer, R., Luo, J. J., Chávez, F., and Shen, Y., "Dynamic Interfacial Tension near Critical Point of a Solvent-antisolvent Mixture and Laminar Jet Stabilization", *Colloid. Surf. A*, **229**(1-3), 181-199 (2003).
17. Lengsfeld, C. S., Delplanque, J. P., Barocas, V. H., and Randolph, T.W., "Mechanism Governing Microparticle Morphology during Precipitation by a Compressed Antisolvent: Atomization vs. Nucleation and Growth", *J. Phys. Chem. B*, **104**(12), 2725-2735 (2000).
18. King, R. P., "Measurement of Particle Size Distribution by Image Analyser", Powder Techn*ol.*, **39**(2), 279–289 (1984).
19. Li, G., Chu, J., Song, E., Row, K. H., Lee, K., and Lee, Y.-W. "Crystallization of Acetaminophen Micro-particle Using Supercritical Carbon Dioxide," *Korean J. Chem. Eng.*, **23**(3), 482-487 (2006).